

Analytical Methods

Accepted Manuscript



This is an *Accepted Manuscript*, which has been through the Royal Society of Chemistry peer review process and has been accepted for publication.

Accepted Manuscripts are published online shortly after acceptance, before technical editing, formatting and proof reading. Using this free service, authors can make their results available to the community, in citable form, before we publish the edited article. We will replace this *Accepted Manuscript* with the edited and formatted *Advance Article* as soon as it is available.

You can find more information about *Accepted Manuscripts* in the [Information for Authors](#).

Please note that technical editing may introduce minor changes to the text and/or graphics, which may alter content. The journal's standard [Terms & Conditions](#) and the [Ethical guidelines](#) still apply. In no event shall the Royal Society of Chemistry be held responsible for any errors or omissions in this *Accepted Manuscript* or any consequences arising from the use of any information it contains.

1
2
3
4
5
6
7
8
9
10
11
12
13
14
15
16
17
18
19
20
21
22
23
24
25
26
27
28
29
30
31
32
33
34
35
36
37
38
39
40
41
42
43
44
45
46
47
48
49
50
51
52
53
54

1 **A novel fluorescent sensor for mercury (II)**
2 **ion using self-assembly of poly (diallyl**
3 **dimethyl ammonium) chloride**
4 **functionalized CdTe quantum dots**

5 Ran Yang^{*a}, Xiaojie Ding^a, Yuchen Zhou^a, Jianjun Li^a, Lingbo Qu^{a,b}, Kangyi Zhang^{*1}

6 ^aThe College of Chemistry and Molecular Engineering, Zhengzhou University,
7 Zhengzhou 450001, PR China

8 ^bSchool of Chemistry & Chemical Engineering, Henan University of Technology,
9 Zhengzhou 450001, PR China

10

55
56
57
58
59
60

* Corresponding author 1: Ran Yang, E-mail: yangran@zzu.edu.cn

Corresponding author 2: KangYi Zhang, E-mail: zhangkangyi@zzu.edu.cn

1
2
3
4
5
6
7
8
9
10
11
12
13
14
15
16
17
18
19
20
21
22
23
24
25
26
27
28
29
30
31
32
33
34
35
36
37
38
39
40
41
42
43
44
45
46
47
48
49
50
51
52
53
54
55
56
57
58
59
60

11 **Abstract**

12 Poly (diallyl dimethyl ammonium) chloride (PDDA) functionalized
13 CdTe quantum dots (QDs) (PDDA-CdTe QDs) was synthesized through
14 the electrostatic self-assembly and used as fluorescence sensor. Mercury
15 (II) ion (Hg^{2+}) has a dramatic fluorescence quenching effect on the
16 PDDA-CdTe QDs. Based on such a quenching effect, a very sensitive
17 fluorescence sensor for Hg^{2+} detection was established. Under the
18 optimum conditions, the fluorescence quenching effect of PDDA-CdTe
19 QDs was linear with the concentration of Hg^{2+} at the range from 0.006
20 μmolL^{-1} to 1.0 μmolL^{-1} . The detection limit was calculated as 5.0 nmolL^{-1}
21 according to the 3σ IUPAC criteria. This PDDA-CdTe QDs sensor system
22 represents a new feasibility to improve the spectroscopic characterization
23 of the QDs sensor to Hg^{2+} .

24 Keywords: CdTe QDs; mercury (II) ion; fluorescent sensor; poly (diallyl
25 dimethyl ammonium) chloride

26

1. Introduction.

Mercury (II) (Hg^{2+}) is a soluble, widespread and dangerous pollutant in water.^{1,2} Under the action of microorganism, inorganic mercury ion will be converted into methyl mercury, which can easily be absorbed by bacteria, plankton and fishes. After accumulating and transforming through the food chain, mercury will causes brain damage, chronic diseases, and lethal effects on human health even at very low concentrations.^{3,4} Therefore, the permissible Hg^{2+} levels set by World Health Organization (WHO) and United States Environmental Protection Agency (USEPA) for drinking water are 5 nmolL^{-1} and 10 nmolL^{-1} ,⁵ respectively. Thus, developing sensitive methods for the quantification of Hg^{2+} at ultra-trace levels in water are very urgent.

To date, a number of conventional methods based on instrumental technologies have been developed for the detection of Hg^{2+} , including fluorescence spectrometry,⁶ colorimetry,⁷ ultrasensitive stripping voltammetry,⁸ atomic emission spectrometry,⁹ atomic absorption spectroscopy,¹⁰ hyper Rayleigh scattering (HRS),¹¹ electrochemistry,¹² inductively coupled plasma mass spectrometry (ICPMS),¹³ and atomic fluorescence spectrometry.¹⁴ Among the reported techniques, fluorescence methods for Hg^{2+} detection have been developed rapidly because of their inherent cheapness, ease of use, facility, high stability and sensitivity.

Quantum dots (QDs), as a new class of fluorescent probes, have

1
2
3
4 49 attracted considerable attention in recent years due to their unique
5
6 50 properties,¹⁵ including narrow, symmetrical and size-tunable emission
7
8
9 51 spectrum, broad excitation spectrum and so on. Cd-chalcogenide
10
11 52 QDs-based nanosensors are widely used in the determination of heavy
12
13 53 metal ions based on the quenching or enhancement of fluorescence
14
15
16 54 intensity of QDs.¹⁶⁻¹⁹ In Xia's paper,²⁰ except Hg^{2+} , Cu^{2+} and Ag^+ could
17
18 55 also quench Cd-chalcogenide QDs, however, different mechanisms have
19
20
21 56 been proposed to explain the quenching effect. Cu^{2+} and Ag^+ quench the
22
23 57 QDs because they bind to the QDs core and facilitate non-radiative
24
25 58 electron/hole recombination annihilation; the quenching mechanism of
26
27 59 Hg^{2+} may be complex: ion-binding and electron transfer, but the latter
28
29 60 effect may play a leading role. Therefore, selective detection of Hg^{2+} and
30
31 61 elimination the interference of Cu^{2+} and Ag^+ could be achieved by means
32
33 62 of using proper method to prevent the contact between metal cations and
34
35 63 QDs core. With this thought, surface-functionalized QDs are employed.
36
37
38
39 64 Tao et al. used QDs functionlized with diethyldithiocarbamate, dithizone,
40
41 65 xylenol orange and rhodanine for the determination of Cu^{2+} , Pb^{2+} and
42
43 66 Ag^+ .²¹⁻²⁴ These functionalized QDs showed good selectivity to the
44
45 67 analytes. Li et al. synthesized chemically denatured ovalbumin
46
47 68 functionalized CdTe QDs which showed high selectivity to Hg^{2+} with a
48
49 69 detection limit of 4.0 nM.²⁵

50
51
52
53
54
55
56 70 Poly (diallyl dimethylammonium) chloride (PDDA), a water-soluble
57
58
59
60

1
2
3
4 71 quaternary ammonium polyelectrolyte, was widely used in water
5
6 72 treatment, paper manufacturing, and the mining industry, as well as in
7
8
9 73 biological applications.²⁶ It contains many positively charged quaternary
10
11 74 ammonium ion which makes it easily assembled with electronegative
12
13 75 mercaptan carboxylic acid capped QDs through the electrostatic
14
15
16 76 self-assembly. Therefore, in this work, the PDDA functionalized TGA
17
18 77 capped CdTe QDs (PDDA-CdTe QDs) were prepared through
19
20
21 78 self-assembly method and used as the fluorescence sensor for the
22
23 79 determination of Hg²⁺. The established method not only was very
24
25
26 80 sensitive with a detection limit of 5.0 nM, but also could effectively
27
28
29 81 eliminate the interference of Cu²⁺ and Ag⁺ and showed good selectivity to
30
31
32 82 Hg²⁺, suggesting a new feasibility to improve the spectroscopic
33
34 83 characterization of the QDs sensor to Hg²⁺.

36 84 **2. Experimental section.**

38 85 **2.1. Materials and chemicals**

40
41 86 All chemicals were of analytical grade and used without further
42
43 87 purification and prepared with double distilled water (DDW). Poly
44
45 88 (diallyl dimethylammonium) chloride, sodium borohydride, thioglycolic
46
47 89 acid (TGA), CdCl₂·2.5H₂O, HgCl₂, Pb(NO₃)₂, AgNO₃, CuCl₂ and other
48
49 90 chemicals were purchased from Sigma-Aldrich. Stock solution of PDDA
50
51 91 (0.005%) was prepared by diluting 35% original PDDA with DDW. 0.05
52
53
54 92 molL⁻¹ phosphate buffer solution (PBS) was prepared with Na₂HPO₄ and
55
56
57
58
59
60

1
2
3
4 93 NaH_2PO_4 .

5
6 94 **2.2. Apparatus**

7
8 95 Absorption spectra of samples were acquired on a Shimadzu
9 96 UV-2550s Spectrophotometer. All fluorescence measurements were
10 97 recorded using a VARIAN Cary Eclipse fluorescence spectrophotometer
11 98 with both excitation and emission slits set at 10.0 nm. Dilute solutions of
12 99 QDs in aqueous medium were placed in 1 cm quartz cuvettes to scan the
13 100 spectrum. The atomic force microscope (AFM) was the Agilent 5500
14 101 model (Aijian Nanotechnology, USA) in tapping mode. All pH
15 102 measurements were made with a pHs-3 digital pH-meter (Shanghai Lei
16 103 Ci Device Works, Shanghai, China) with a combined glass electrode. All
17 104 optical measurements were performed at room temperature and under
18 105 ambient conditions.

19 20
21 22 23 24 25 26 27 28 29 30 31 32 33 34 35 36 37 38 39 40 41 42 43 44 45 46 47 48 49 50 51 52 53 54 55 56 57 58 59 60
106 **2.3. Preparation of PDDA functionalized CdTe QDs**

107 TGA capped CdTe QDs were synthesized according to the published
108 method with some modifications.²⁷ In brief, 1.0 mmol (0.1276 g)
109 tellurium (Te) powder, 3.0 mmol (0.1135 g) sodium borohydride and 4.0
110 mL ultrapure water were added into a clear flask in an ice-bath. Until the
111 black Te powder completely reacted, the purple transparent NaHTe
112 solution was obtained. The fresh NaHTe solution was added to CdCl_2
113 aqueous solution at a pH of 10.0 in the presence of TGA under nitrogen.
114 The molar ratio of $\text{Te}^{2-}/\text{Cd}^{2+}/\text{TGA}$ was fixed at 1:2:5.7. After refluxed at

1
2
3
4 115 95 °C for different time (1.0, 2.0, 3.0, 3.5 h), the solution was precipitated
5
6 116 by ethanol with centrifugation at 10000 rpm for 5 min. Then the
7
8 117 precipitation were dissolved in DDW and used in the experiment.
9
10 118 According to the Te^{2-} concentration, the concentration of colloidal
11
12 119 quantum dots was 0.01 M.
13
14

15
16 120 PDDA functionalized CdTe QDs were prepared by adding 70 μL of
17
18 121 0.005% PDDA to 20 μL of 0.01 mol L^{-1} TGA-CdTe QDs, subsequently
19
20 122 diluted with DDW.
21
22

23 123 **2.4 Procedure for the fluorescence measurement of Hg^{2+}**

24
25 124 To a series of 10.0 mL colorimetric tube, 20 μL of 0.01 molL^{-1}
26
27 125 TGA-CdTe QDs, 70 μL of 0.005% PDDA solution, 50 μL of 0.05 molL^{-1}
28
29 126 PBS buffer (pH 6.5), 10 μL of 1.0 molL^{-1} NaCl solution and appropriate
30
31 127 amount of Hg^{2+} stock solution were sequentially added. The mixture was
32
33 128 diluted with DDW to 3.00 mL and mixed thoroughly for measurements
34
35 129 after 20 min. The fluorescence intensity was measured at
36
37 130 $\lambda_{em}/\lambda_{ex}=528/350$ nm.
38
39

40 131 **3. Results and discussion**

41 132 **3.1. Characterization of the TGA capped CdTe QDs**

42
43 133 As shown in **Fig. 1**, all the fluorescence emission spectra were
44
45 134 symmetrical and narrow, indicating the prepared QDs were nearly
46
47 135 homogeneous and monodisperse.²⁸ According to the following formula
48
49 136 (1),²⁹ the diameter of different nanocrystals with different refluxing time
50
51
52
53
54
55
56
57
58
59
60

1
2
3
4 137 of 1.0 h, 2.0 h, 3.0 h, 3.5 h were 0.78 nm, 1.31 nm, 1.76 nm, 1.87 nm,
5
6 138 respectively. These were in accordance with the reported papers that the
7
8
9 139 particle size of QDs increased with the refluxing time.³⁰

10
11 140
$$D = (9.8127 \times 10^{-7}) \lambda^3 - (1.7147 \times 10^{-3}) \lambda^2 + (1.0064) \lambda - 194.84 \quad (1)$$

12
13
14 141 where λ is the maximum absorption of CdTe QDs.

15 142 **3.2. Characterization of PDDA-CdTe QDs**

16
17
18
19 143 As shown in **Fig.2A**, with the addition of PDDA, UV-vis absorption
20
21 144 spectra and fluorescence emission spectra of CdTe QDs changed with
22
23
24 145 enhancement and red-shift. Those changes indicated the interaction
25
26 146 between PDDA and CdTe QDs.

27
28
29 147 To understand the effect of PDDA on the colloidal stability of CdTe
30
31 148 QDs, the zeta potential of CdTe QDs and PDDA-CdTe QDs in PBS
32
33
34 149 buffer (pH=6.5) was investigated. The initial value of zeta potential of
35
36 150 CdTe QDs was -23.2 mV, which suggested relatively stable suspensions.
37
38
39 151 After the addition of PDDA, the zeta potential value of CdTe QDs was
40
41 152 only -4.65 mV, which suggested unstable suspensions. With addition of
42
43
44 153 PDDA, decrease of stability of CdTe QDs may be attributed to the
45
46 154 aggregation of CdTe QDs. To confirm this assumption, the AFM of CdTe
47
48
49 155 QDs and PDDA-CdTe QDs were studied. From **Fig.2B a** and **b**, it could
50
51 156 be seen that after addition of PDDA, CdTe QDs aggregated obviously,
52
53
54 157 which was accordance with the self-assembly of CdTe QDs and CTAB.³¹

55
56
57 158 At the experimental pH (6.5), PDDA is positive, the TGA capped CdTe
58
59
60

1
2
3
4 159 QDs are negatively charged. It is very easy for them to interaction
5
6 160 through electrostatic interaction. To prove such assumption, the effect of
7
8
9 161 ionic strength on the interaction of CdTe QDs and PDDA was
10
11 162 investigated by adding NaCl (0.05 M) into the system. With the addition
12
13 163 of NaCl, fluorescence enhancement of PDDA to CdTe QDs decreased
14
15
16 164 rapidly (**Fig.2C**). It suggested the electrostatic interaction between them,
17
18 165 because the ionic strength in solution has a diminishing effect on the
19
20
21 166 electrostatic interaction between two molecules.³²
22
23

24 167 The above results from spectra, zeta potential and AFM indicated that
25
26 168 with the addition of PDDA, the CdTe QDs aggregated through
27
28
29 169 electrostatic interaction.
30

31 170 **3.3. Factors that affect the sensing of PDDA-CdTe QDs for Hg²⁺**

32
33
34 171 To achieve better sensing for Hg²⁺, the experiments conditions
35
36 172 including size of CdTe QDs, the ratio of PDDA to CdTe QDs, the reaction
37
38
39 173 pH, ionic strength and reaction time were optimized according to the
40
41 174 fluorescence quenching efficiency (F_0/F) of CdTe QDs toward Hg²⁺,
42
43
44 175 where, F_0 and F are fluorescence intensity of the PDDA-CdTe QDs in the
45
46 176 absence and presence of Hg²⁺, respectively.
47

48 49 177 **3.3.1 Effect of size of CdTe QDs on the detection of Hg²⁺**

50
51 178 From the work of Rodrigues,³³ sizes of QDs showed a strong effect on
52
53
54 179 the sensitivity of the fluorescence methodology. CdTe QDs with the
55
56 180 diameter of 0.78, 1.31, 1.76, 1.87 nm, functioned with PDDA revealed
57
58
59
60

1
2
3
4 181 different sensitivity to Hg^{2+} (**Fig.3A**). It can be seen that the PDDA-CdTe
5
6 182 QDs with the diameter of 1.76 nm of QDs showed the best sensitivity to
7
8
9 183 Hg^{2+} . So, in the following experiments, CdTe QDs with the diameter of
10
11 184 1.76 nm were used.

14 185 **3.3.2 The ratio of PDDA to CdTe QDs on Hg^{2+} detection**

16 186 According to the synthesis procedure, different PDDA-CdTe QDs were
17
18 187 prepared by adding different volume of 0.005% PDDA into 20 μL 0.01
19
20 188 molL^{-1} CdTe QDs solution and subsequently diluted with DDW to 3.00
21
22 189 mL. With the increasing of volume of PDDA, the fluorescence intensity
23
24 190 of formed PDDA-CdTe QDs increased greatly, and the maximum
25
26 191 fluorescence intensity was obtained at the addition of 70 μL PDDA (**Fig.**
27
28 192 **3B**). Furthermore, at this concentration of PDDA (70 μL of 0.005 %), the
29
30 193 fluorescence quenching efficiency (F_0/F) also reached the maximum (inset
31
32 194 of **Fig. 3B**). Therefore, the optimal usage of PDDA for the self-assembly
33
34 195 with CdTe QDs were kept at 70 μL 0.005% PDDA to 20 μL 0.01 M
35
36 196 TGA-CdTe QDs.

44 197 **3.3.3 Effect of pH and ionic strength**

46 198 The surface state of capped molecule TGA changed with different pH,
47
48 199 which will affect the electrostatic interaction between PDDA and
49
50 200 TGA-CdTe QDs. So, the effect of solution pH was investigated by adding
51
52 201 a series of 0.05 molL^{-1} PBS with different pH into the reaction system
53
54 202 (**Fig.3C**). The maximum fluorescence quenching efficiency occurred at
55
56
57
58
59
60

1
2
3
4 203 pH 6.5. Thus, 50 μL PBS (pH 6.5) was recommended for used in this
5
6 204 work.

7
8
9 205 As depicted in **Section 3.2**, addition of NaCl makes an important
10
11 206 influence on the interaction between PDDA and CdTe QDs, which yields
12
13 207 in a corresponding effect on sensing of PDDA-CdTe QDs. So, the effect
14
15 208 of ionic strength on the interaction of PDDA-CdTe QDs and Hg^{2+} was
16
17 209 also investigated as shown in **Fig.3D**. It can be seen that the optimum
18
19 210 ionic strength is adding 10 μL 0.1 M NaCl into reaction system (the final
20
21 211 concentration was 3.3 mM).

22 212 **3.3.4 Effect of reaction time on the detection of Hg^{2+}**

23
24
25
26
27
28
29 213 The reaction time between PDDA-CdTe QDs and Hg^{2+} was
30
31 214 investigated on the variation of fluorescence intensity along with the time.
32
33 215 For PDDA-CdTe QDs with different Hg^{2+} concentration, the fluorescence
34
35 216 intensity was recorded every 5 min (**Fig.3E**). According to the
36
37 217 experimental results, the reaction between Hg^{2+} and PDDA-CdTe QDs
38
39 218 reached equilibrium in about 20 min, and the fluorescence intensity was
40
41 219 stable for at least 40 min at room temperature. Thus, 20 min reaction time
42
43 220 was selected for the reaction time between PDDA-CdTe QDs and Hg^{2+} .

44 221 **3.4 Selectivity of fluorescence assay for Hg^{2+}**

45
46
47
48
49 222 To investigate the selectivity of the PDDA-CdTe QDs towards Hg^{2+} ,
50
51 223 the fluorescence intensity of PDDA-CdTe QDs in the 0.2 μM Hg^{2+} and
52
53 224 other metal ions (Pb^{2+} , Ag^+ , Cu^{2+} , Mn^{2+} , Co^{2+} , Ni^{2+} , Fe^{3+} , Mg^{2+} , Zn^{2+} , Al^{3+} ,

1
2
3
4 225 Na⁺) were studied (**Fig. 4**). It can be seen that at the same concentration
5
6 226 (0.2 μM), the quenching effect of QDs caused by other metal ions was
7
8
9 227 still not beyond 7%, which was much smaller than that caused by Hg²⁺.
10
11 228 Relative to the crude CdTe QDs without modification,^{27,34} the PDDA-CdTe
12
13 229 QDs can effectively eliminate the interference of Ag⁺ and Cu²⁺ and
14
15
16 230 showed more selectivity for Hg²⁺.

231 **3.5. Analytical performance of PDDA-CdTe QDs**

232 At optimum experimental conditions, the fluorescence spectra of
233 PDDA-CdTe QDs with the addition of different concentrations of Hg²⁺
234 were recorded (**Fig. 5**). The fluorescence quenching efficiency (F_0/F) and
235 the concentration of Hg²⁺ in the range from 0.006 to 1.0 μmolL⁻¹ showed
236 a good linear relationship as $F_0/F = 1.0703 + 4.1253C$ (C: μmolL⁻¹)
237 ($r=0.9985$). The limit of detection (LOD), calculated following the 3σ
238 IUPAC criteria is 5.0 nmolL⁻¹, which is lower than the tolerance limit of
239 10 nmolL⁻¹ for mercury in drinking water permitted by the United States
240 Environmental Protection Agency (USEPA).⁵

241 For comparative purpose, the analytical performance of several
242 selected fluorimetric methods based on QDs for Hg²⁺ detection is
243 summarized in **Table 1**. The proposed PDDA-CdTe QDs sensor possesses
244 comparable or superior linear range, sensitivity.

245 **3.6. The mechanism of reaction**

246 The fluorescence quenching may result from two causes.³⁵ One is

1
2
3
4 247 dynamic quenching which results from the collision between the
5
6 248 fluorophore and a quencher. The other is static quenching which results
7
8
9 249 from the ground-state complex formation between the fluorophore and a
10
11 250 quencher. To ascertain the cause of the quenching, the Stern-Volmer
12
13 251 equation³⁶ was first applied to model the quenching of PDDA-CdTe QDs
14
15
16 252 with respect to Hg^{2+} concentration, it is described as:

17
18
19 253
$$F_0/F = 1 + K_q \tau_0 [Q] = 1 + K_{sv}[Q] \quad (2)$$

20
21 254 For which F_0 and F are the fluorescence intensities in the absence and
22
23 255 presence of the quencher Q , K_q is the quenching rate constant of the
24
25 256 biomolecule, τ_0 is the average life-time of molecule without the quencher
26
27
28 257 and its value is 10^{-8} s. K_{sv} is the Stern-Volmer dynamic quenching
29
30 258 constant. Based on the experimental data, K_q was calculated as 4.2×10^{14} L
31
32 259 $\text{mol}^{-1} \text{S}^{-1}$, which was a factor of four hundred greater than the maximum
33
34 260 scatter collision quenching constant of various other quenchers for the
35
36
37 261 biopolymer ($2.0 \times 10^{10} \text{ Lmol}^{-1} \text{S}^{-1}$).³⁷ This result implies that the
38
39 262 fluorescence quenching arises from the static quenching mechanism.

40
41
42 263 Static quenching the fluorescence of QDs may happen by energy
43
44 264 transfer,³⁸ charge diverting,³⁹ and surface absorption.⁴⁰ In order to
45
46
47 265 investigate the quenching mechanism of fluorescence by Hg^{2+} , UV-Vis
48
49 266 absorption spectra of the interaction between PDDA-CdTe QDs and Hg^{2+}
50
51
52 267 were studied (**Fig. 6**). The results showed no obvious blue-shift or
53
54
55 268 red-shift in the absorption spectra of PDDA-CdTe QDs before and after
56
57
58
59
60

1
2
3
4 269 adding Hg^{2+} . In addition, there was also no significant shift in
5
6 270 fluorescence spectra of PDDA-CdTe QDs caused by Hg^{2+} (**Fig. 5**).
7
8
9 271 Therefore, the quenching phenomenon in this system is possibly
10
11 272 attributed to the effective electron transfer from PDDA to Hg^{2+} (Scheme
12
13 273 1). This implied that, Hg^{2+} effectively quench the fluorescence of
14
15
16 274 PDDA-CdTe QDs facilitating nonradiative recombination of excited
17
18
19 275 electron (e^-) in the conduction bands and holes (h^+) in the valence band.⁴¹

21 276 **3.7 Analysis of samples**

22
23
24 277 To investigate the applicability of the proposed method for the
25
26 278 determination of Hg^{2+} , local lake water sample (obtained from the lake of
27
28
29 279 Zhengzhou University) was used for quantitative analysis. The sample
30
31 280 was filtrated before use. The pH of the sample was detected as 6.39 which
32
33
34 281 was not equal to the optimum pH, so appropriated amount of PBS buffer
35
36 282 was added to the samples to adjust the pH to 6.5. No obvious
37
38
39 283 fluorescence quenching was found for the pretreated lake sample. The
40
41
42 284 recoveries experiments were performed by measuring fluorescence
43
44 285 intensity for samples in which known concentrations of Hg^{2+} were added
45
46 286 to the lake water. The recoveries for Hg^{2+} were ranged from 97.5-103.0%
47
48
49 287 (**Table 2**). These results clearly indicate the applicability and reliability of
50
51
52 288 the proposed method.

54 289 **4. Conclusion.**

55
56 290 In this work, we have demonstrated a novel, sensitive, selective
57
58
59
60

1
2
3
4 291 fluorescent sensor for Hg^{2+} based on PDDA-CdTe QDs, which were
5
6 292 constructed through electrostatic self-assembly between PDDA and CdTe
7
8
9 293 QDs. Compared with CdTe QDs, PDDA-CdTe QDs fluorescent sensor
10
11 294 eliminates the interference of Cu^{2+} and Ag^+ , and possesses comparable or
12
13 295 superior linear range and selectivity to Hg^{2+} . To our best knowledge, it is
14
15
16 296 the first time to apply PDDA-CdTe QDs in Hg^{2+} fluorescence assay.
17

18
19 297 **Reference**

- 20
21 298 1 T. Stoichev and D. Amouroux, *Appl. Spectrosc. Rev.*, 2006, 41,
22
23 299 591–619.
24
25
26 300 2 N. Vasimalai and S. A. John, *Analyst*, 2012, 137, 3349–3354.
27
28
29 301 3 M. Aschner, J.L. Aschner, *Neuroscience and Biobehavioral Reviews*,
30
31 302 1990, 14, 169-176.
32
33
34 303 4 K.V. Gopal, *Neurotoxicol Teratol*, 2003, 25, 69–76.
35
36
37 304 5 E. Álvarez-Ayuso, A. García-Sánchez and X. Querol, *Water Res.*, 2003,
38
39 305 37, 4855–4862.
40
41
42 306 6 D. Liu, S. Wang, M. Swierczewska, X. Huang, A.A. Bhirde, J. Sun, Z.
43
44 307 Wang, M. Yang, X. Jiang and X. Chen, *ACS Nano.*, 2012, 6,
45
46 308 10999–11008.
47
48
49 309 7 H. Wang, Y. Wang, J. Jin and R. Yang, *Anal. Chem.*, 2008, 80,
50
51 310 9021–9028.
52
53
54 311 8 J. Gong, T. Zhou, D. Song and L. Zhang, *Sens. Actuat. B*, 2010, 150,
55
56 312 491–497.
57
58
59
60

- 1
2
3
4 313 9 Z. Zhu, G.C.Y. Chan, S.J. Ray, X. Zhang and G.M. Hieftje, *Anal. Chem.*,
5
6 314 2008, 80, 8622–8627.
7
8
9 315 10 M.A. Domínguez, M. Grünhut, M.F. Pistonesi, M.S. Di Nezio, M.E.
10
11 316 Centurión and J. Agric, *Food Chem.*, 2012, 60, 4812–4817.
12
13
14 317 11 G. K. Darbha, A. K. Singh, U. S. Rai, E. Yu, H. Yu and P. Chandra Ray,
15
16 318 *J. Am. Chem. Soc.*, 2008, 130, 8038–8043.
17
18
19 319 12 Z. Zhu, Y. Su, J. Li, D. Li, J. Zhang, S. Song, Y. Zhao, G. Li and C.
20
21 320 Fan, *Anal. Chem.*, 2009, 81, 7660–7666.
22
23
24 321 13 R. Clough, S.T. Belt, E.H. Evans, B. Fairman and T. Catterick, *Anal.*
25
26 322 *Chim. Acta*, 2003, 50, 155–170.
27
28
29 323 14 H. Bagheri and A. Gholami, *Talanta*, 2001, 55, 1141–1150.
30
31 324 15 K. M. Hanif, R. W. Meulenberg and G. F. Strouse, *J. Am. Chem. Soc.*,
32
33 325 2002, 124, 11495-11502.
34
35
36 326 16 J. Pei, H. Zhua and X. Wang *Anal. Chim. Acta*, 2012, 757, 63-68.
37
38
39 327 17 R. Zhang and W. Chen, *Biosens. Bioelectron.*, 2014, 55, 83–90.
40
41 328 18 M. Koneswaran and R.Narayanaswamy, *Microchim Acta*, 2012, 178,
42
43 329 171-178.
44
45
46 330 19 M. R. Chao, Y. Z. Chang and J. L. Chen, *Biosens. Bioelectron.*, 2013,
47
48 331 42, 397-402.
49
50
51 332
52
53
54 333 20 Y.S. Xia, and C.Q. Zhu, *Talanta*, 2008, 75, 215–221.
55
56
57 334 21 J. Wang, H. Ma and G. Tao, *Spectrochim. Acta A*, 2011, 81, 178–183.
58
59
60

- 1
2
3
4 335 22 Q. Zhao, H. Ma and G. Tao, *J. Hazard. Mater.*, 2013, 250, 45–52.
5
6 336 23 Q. Zhao, H. Ma and G. Tao, *Talanta*, 2013, 114, 110–116.
7
8
9 337 24 L. Chen, Q. Zhao, X. Y. Zhang and G. Tao, *Chinese Chem. Lett.*, 2014,
10
11 338 25, 261–264.
12
13 339 25 Y. Q. Wang, Y. Liu and X. W. He, *Talanta*, 2012, 99: 69-74.
14
15
16 340 26 J.-F. Rochette, E. Sacher, M. Meunier and J. H. T. Luong, *Anal.*
17
18 341 *Biochem.*, 2005, 336, 305-311.
19
20
21 342 27 M. H. Sorouraddin, I. N. Amin, *J. Lumin.* 2014, 145, 253–258.
22
23
24 343 28 C.R. Tanga, Z. Sua and B.G. Lin, *Anal. Chim. Acta*, 2010, 678,
25
26 344 203–207.
27
28
29 345 29 O. Adegoke and T. Nyokong, *J. Lumin.*, 2013, 134, 448-455.
30
31 346 30 M. Gao, S. Kirstein, H. Mhwald, A.L. Rogach, A. Kornowski, A.
32
33 347 Eychmlller and H. Weller, *J. Phys. Chem. B*, 1998, 102, 8360-8363.
34
35
36 348 31 J.R. Lakowicz, Plenum Press, New York, 1983.
37
38
39 349 32 X.L. Diao, Y.S. Xia, T.L. Zhang, Y. Li and C.Q. Zhu, *Anal. Bioanal.*
40
41 350 *Chem.*, 2007, 388, 1191–1197.
42
43
44 351 33 S. Sofia M. Rodrigues and Adriana S. Lima, *Fuel*, 2014, 117, 520–527.
45
46 352 34 Y. S. Xia and C.Q. Zhu, *Talanta*, 2008, 75, 215–221.
47
48
49 353 35 B. Wang, S. Zhuo, L. Chen and Y. Zhang, *Spectrochim. Acta, Part A*,
50
51 354 2014, 131, 384 – 387.
52
53
54 355 36 J. R. Lakowicz and G. Weber, *Biochem.*, 1973, 12, 4161-4170.
55
56 356 37 P. K. Behera, T. Mukherjee and A. K. Mishra, *J. Lumin.*, 1995, 65,
57
58
59
60

1
2
3
4 357 131-136.
5

6 358 38 J. Tang and R. A. Marcus, *J. Chem. Phys.*, 2006, 125, 44703.
7

8 359 39 X. J. Ji, J. Y. Zheng and J. M. Xu, *J. Phys. Chem. B*, 2005, 109,
9

10 360 3793-3799.
11

12 361 40 C. Q. Dong, H. F. Qian, N. H. Fang and J. C. Ren, *J. Phys. Chem. B*,
13

14 362 2006, 110, 11069-11075.
15

16 363 41 C. Landes, C. Burda, M. Braun and M.A. El-Sayed, *J. Phys. Chem. B*,
17

18 364 2001, 105, 2981–2986.
19

20 365
21
22
23
24
25
26
27
28
29
30
31
32
33
34
35
36
37
38
39
40
41
42
43
44
45
46
47
48
49
50
51
52
53
54
55
56
57
58
59
60

366 Table 1 Comparison of the linear range and detection limit of QDs-based sensing
 367 systems for determination of Hg²⁺

sensors	Linear range ($\mu\text{mol L}^{-1}$)	LOD ($\mu\text{mol L}^{-1}$)	Ref.
CA coated CdTe QDs	0.08 -3.33	0.07	16
nitrogen-doped carbon QDs	0-25	0.23	17
MAA capped CdS/ZnS QDs	0.0025 -0.28	0.0022	18
EMIDCA passivated TGA capped CdTe QDs	0.23-53	0.23	19
dOB coated CdTe QDs	0.008 – 3.0	0.0042	25
dBSA-coated CdTe QDs	0.012 -1.5	0.004	34
Graphene QDs	0.80-9.0	0.10	35
PDDA functionalized CdTe QDs	0.006-1.0	0.005	This work

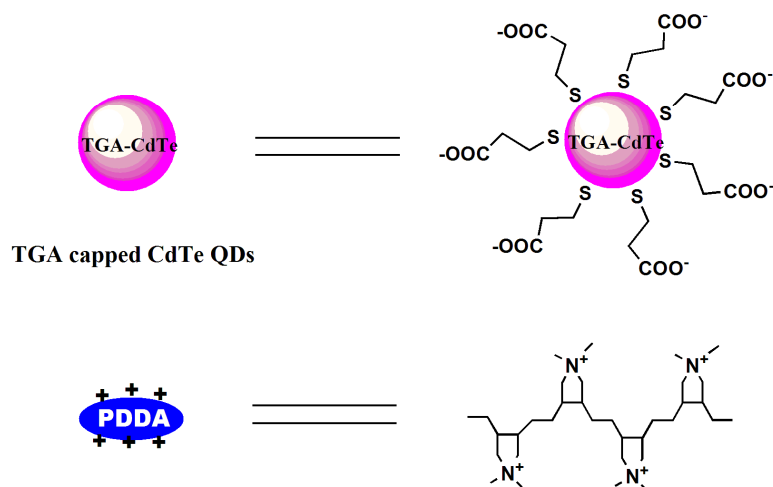
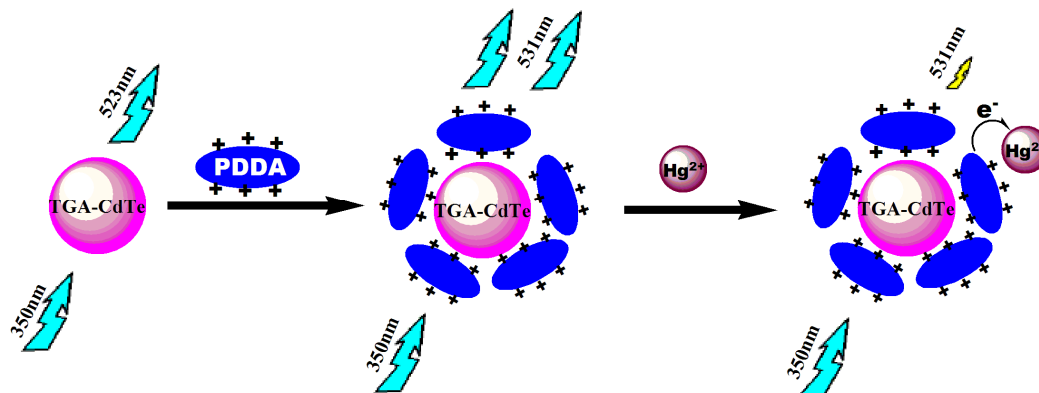
368 QDs: quantum dots; CA: cysteamine; MAA: mercaptoacetic acid; EMIDCA:
 369 1-ethyl-3-methylimidazolium dicyanamide; TGA: thioglycolic acid; dOB: denatured
 370 ovalbumin; dBSA: denatured bovine serum albumin;

371 Table 2 Analytical results for the detection of Hg^{2+} in spiked lake water sample (n=5)

Samples	Added standard solution (molL^{-1})	Found total value (molL^{-1})	RSD (%)	Recovery (%)
1	2.0×10^{-8}	1.95×10^{-8}	1.06	97.5
2	1.0×10^{-7}	1.03×10^{-7}	1.15	103.0
3	8.0×10^{-7}	8.09×10^{-7}	1.14	101.1

372

A novel fluorescent sensor was constructed to selective quantitatively analysis of mercury (Hg^{2+}) ion, based on self-assembly of poly (diallyl dimethyl ammonium) chloride functionalized CdTe quantum dots.



Scheme 1. The schematic illustration for mercury sensing based on PDDA-CdTe QDs fluorescence system.

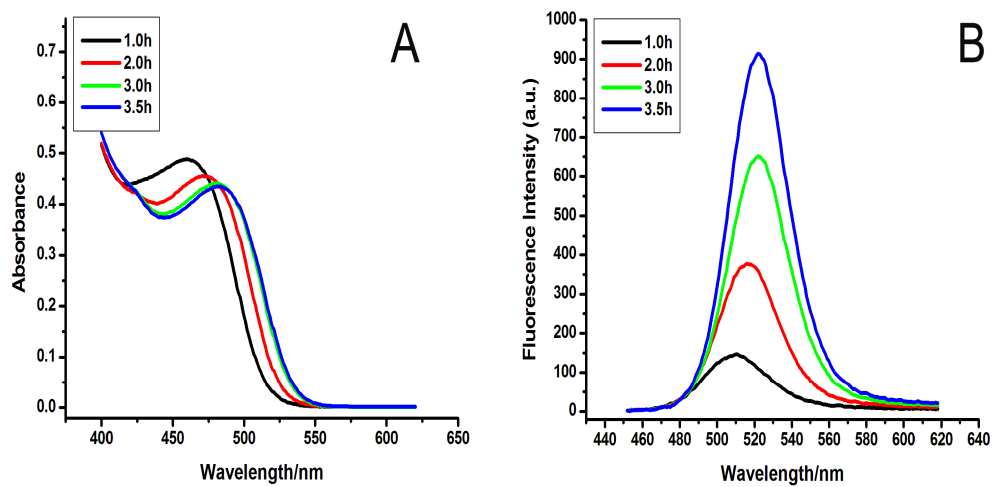


Fig.1

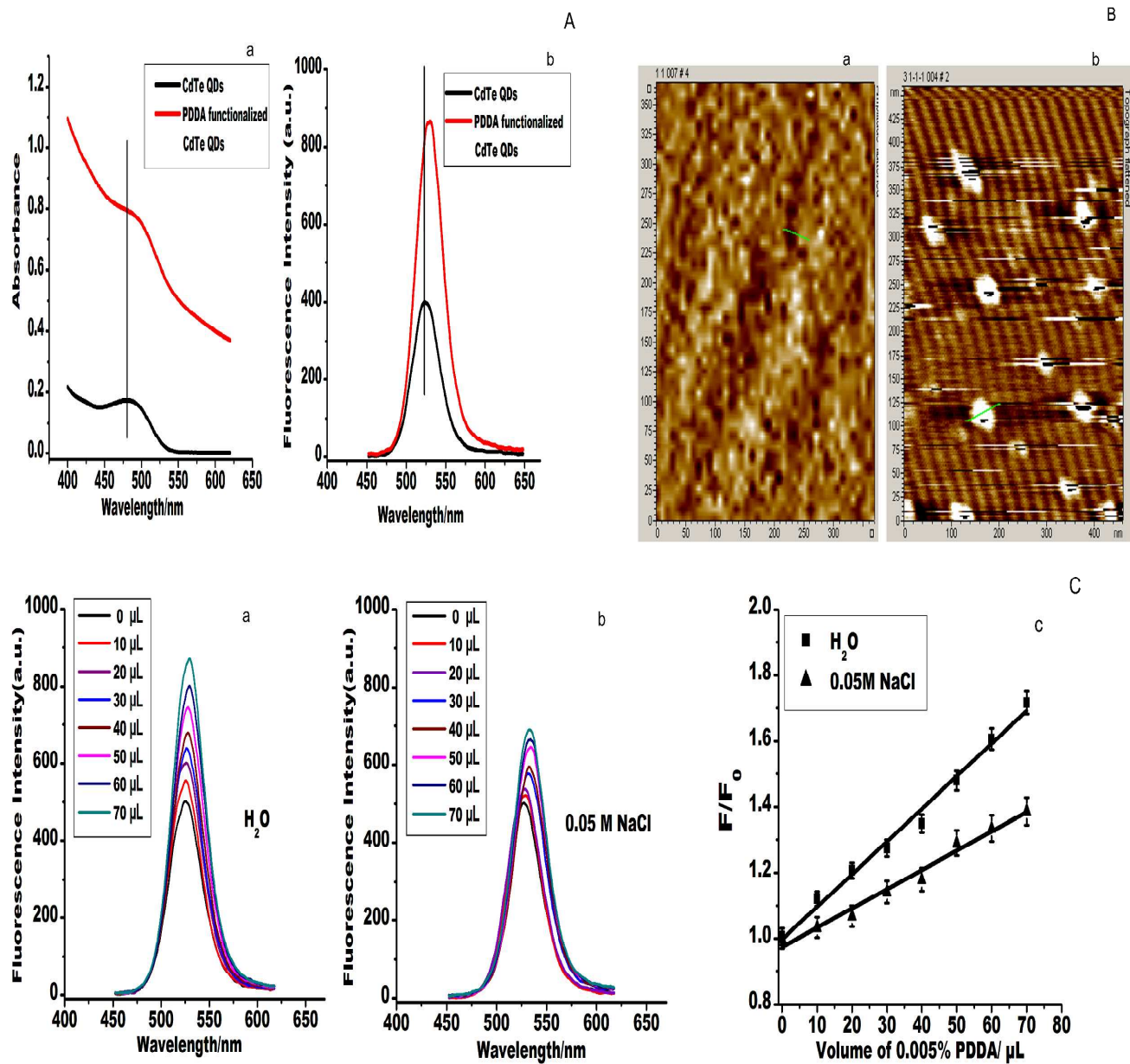


Fig.2

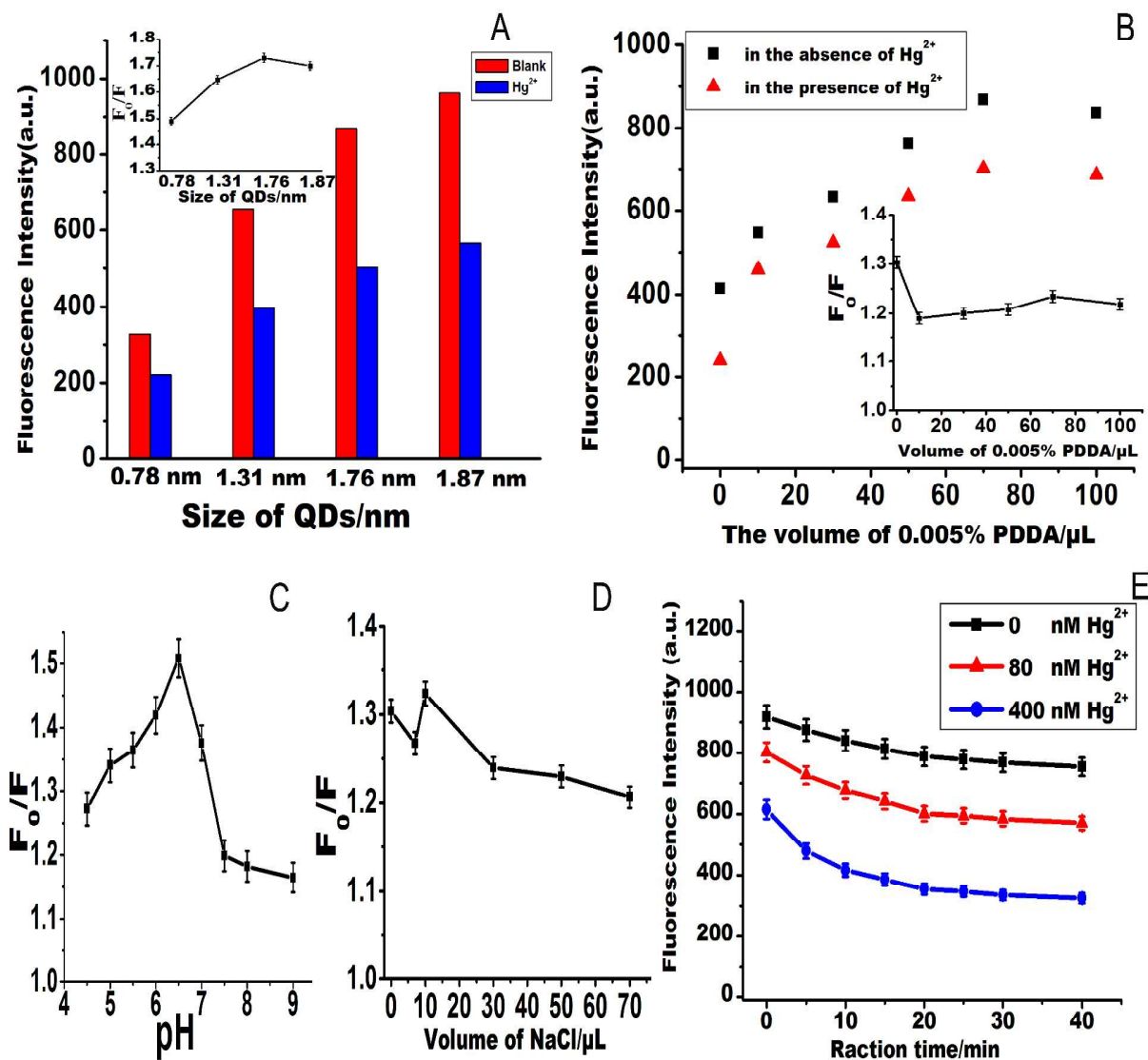


Fig.3

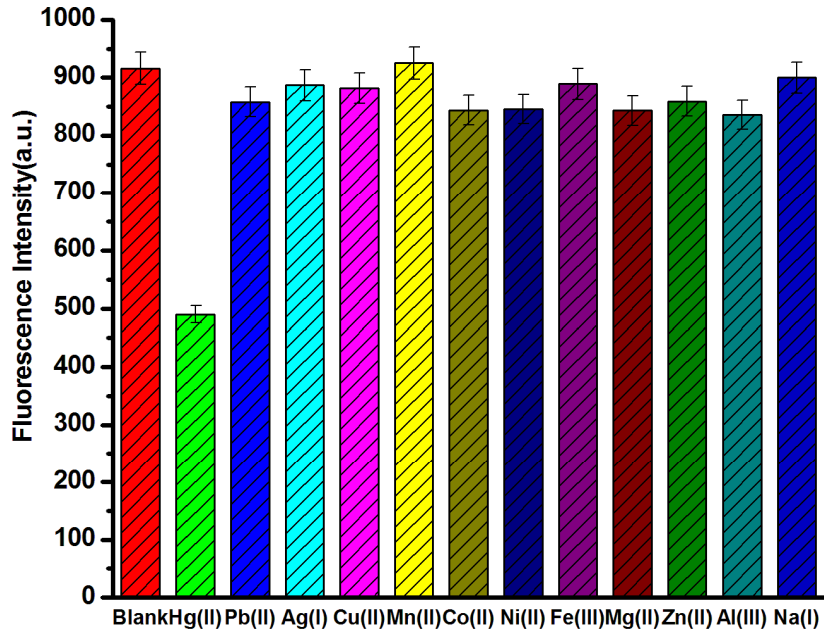


Fig.4

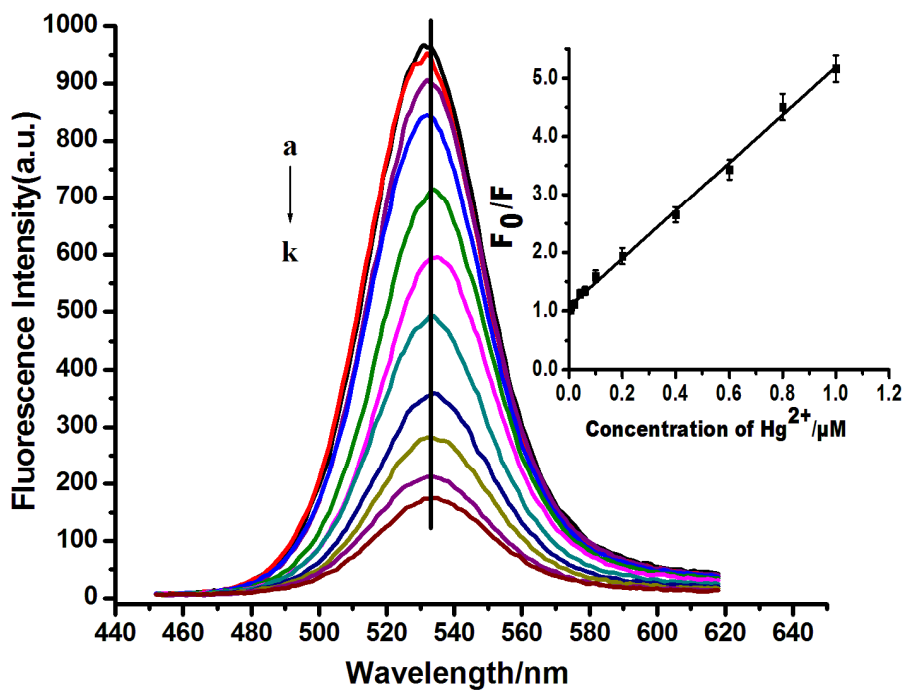


Fig.5

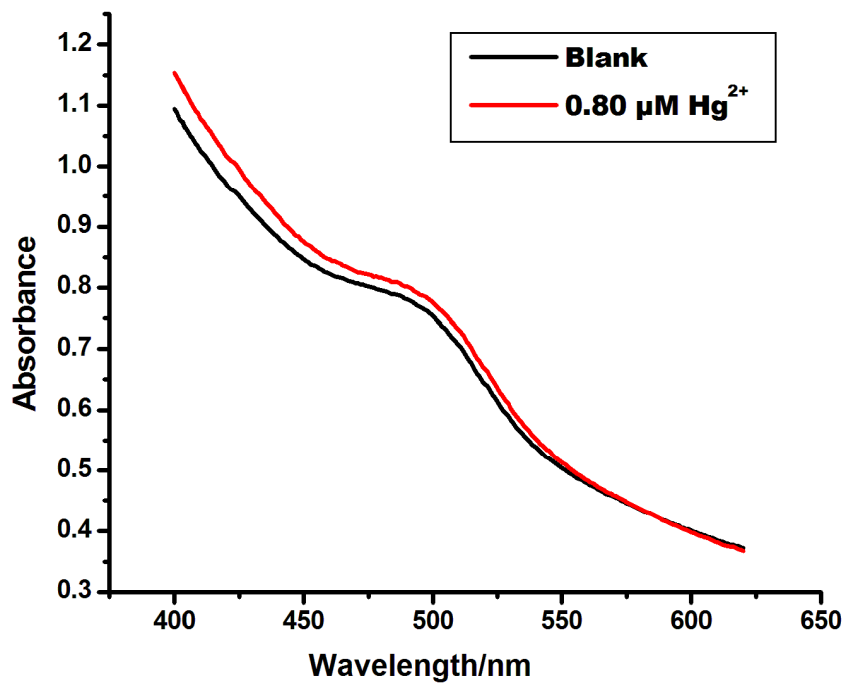


Fig.6

1
2
3
4
5
6
7
8
9
10
11
12
13
14
15
16
17
18
19
20
21
22
23
24
25
26
27
28
29
30
31
32
33
34
35
36
37
38
39
40
41
42
43
44
45
46
47
48
49
50
51
52
53
54
55
56
57
58
59
60

1
2
3
4 Fig.1 (A) Absorption spectrum of the CdTe QDs (5.0 mmolL^{-1}); (B) Fluorescence emission
5
6 spectra of the CdTe QDs (1.0 mmolL^{-1}).
7
8
9

10
11 Fig.2 (A) Absorption spectrum of CdTe QDs and PDDA-CdTe QDs (a); Fluorescence emission
12
13 spectra of CdTe QDs and PDDA-CdTe QDs (b); (B) AFM images of CdTe QDs (a) and
14
15 PDDA-CdTe QDs (b); (C) Fluorescence spectra of PDDA-CdTe QDs with different concentration
16
17 of PDDA in H_2O (a) and 0.05 molL^{-1} NaCl solution (b); plot of the fluorescence enhancement of
18
19 CdTe QDs by PDDA in H_2O and 0.05 molL^{-1} (c).
20
21
22
23
24
25

26 Fig.3 (A) Effect of sizes of CdTe QDs on sensitivity of Hg^{2+} ; inset is the F_0/F vs refluxed time of
27
28 CdTe QDs; (B) Effect of concentration of PDDA on fluorescence intensity of the PDDA-CdTe
29
30 QDs and Hg^{2+} system; inset is the F_0/F vs pH plot; (C) Effect of pH on the detection of Hg^{2+} ; (D)
31
32 Effect of concentration of NaCl on sensitivity of Hg^{2+} ; (E) Effect of reaction time on the detection
33
34 of Hg^{2+} .
35
36
37
38
39
40

41 Fig.4 Effect of different metal ions ($0.2 \text{ }\mu\text{molL}^{-1}$) on the fluorescence intensity of PDDA-CdTe
42
43 QDs.
44
45
46
47
48

49 Fig.5 The fluorescence response of CA-CdTe QDs to addition of various concentration of Hg^{2+} ;
50
51 inset is the F_0/F vs c plot (the concentrations of Hg^{2+} from a to k: $0 \text{ }\mu\text{molL}^{-1}$; $0.006 \text{ }\mu\text{molL}^{-1}$; 0.008
52
53 μmolL^{-1} ; $0.02 \text{ }\mu\text{molL}^{-1}$; $0.06 \text{ }\mu\text{molL}^{-1}$; $0.1 \text{ }\mu\text{molL}^{-1}$; $0.2 \text{ }\mu\text{molL}^{-1}$; $0.4 \text{ }\mu\text{molL}^{-1}$; $0.6 \text{ }\mu\text{molL}^{-1}$; 0.8
54
55 μmolL^{-1} ; $1.0 \text{ }\mu\text{molL}^{-1}$).
56
57
58
59
60

Fig.6 Absorption spectrum before of Hg^{2+} and after addition of Hg^{2+} .

1
2
3
4
5
6
7
8
9
10
11
12
13
14
15
16
17
18
19
20
21
22
23
24
25
26
27
28
29
30
31
32
33
34
35
36
37
38
39
40
41
42
43
44
45
46
47
48
49
50
51
52
53
54
55
56
57
58
59
60